Tomasz RYMARCZYK[1,2], Andres VEJAR[1,2]

Research & Development Centre Netrix S.A.(1), University of Economics and Innovation (2)

Waveform-Reconfigurable Emitter Design for Multi Frequency Electrical Tomography

Abstract. In this work we present a design of a multi-frequency electrical tomography (ET) data acquisition device focused on reconfiguration of the emitter for on-line customization of excitation signals. The design is conceived to acquire data for in vivo medical monitoring. This device is implemented using FPGA for real-time data acquisition and a microcontroller SoC that enables internet of things capabilities for further escalation of the device functionality. The ET device allow the study of frequency responses and the generation of customized excitation signals.

Streszczenie. W niniejszej pracy przedstawiamy projekt urządzenia do akwizycji danych z wieloczęstotliwościowej tomografii elektrycznej (ET), którego celem jest rekonfiguracja emitera w celu dostosowania sygnałów wzbudzenia w trybie online. Projekt ma na celu pozyskiwanie danych do monitorowania medycznego in vivo. Urządzenie zostało zaimplementowane przy użyciu FPGA do akwizycji danych w czasie rzeczywistym oraz mikrokontrolera SoC, w celu dalszego zwiększenia funkcjonalności urządzenia. Urządzenie ET umożliwia badanie odpowiedzi częstotliwościowych i generowanie niestandardowych sygnałów pobudzających. (Konstrukcja nadajnika z rekonfigurowalnym kształtem fali dla wieloczęstotliwościowej tomografii elektrycznej).

Keywords: electrical tomography; sensors, FPGA, internet of things.
Słowa kluczowe: tomografia elektryczna; sensory, FPGA; internet rzeczy.

Introduction

The process of data acquisition for in vivo electrical tomography (ET) is a non-trivial operation given the complex structure of life tissue nand the natural occurrence of electrochemical activity. In the case of medical ET imaging, the most important task is to provide functional information of the subject under study: lung function monitoring and cardiopulmonar monitoring being the most significant applications.

The skin tissue interface presents a layered cell composition that acts as a natural barrier for electrical stimulation and sensing, fundamental processes behind ET data acquisition. Taking into account the fact that for medical safety reasons the excitation signal is energy-constrained, the incorporation of frequency and waveform exploration capabilities into the design of medical ET excitation emitters is an essential task. The prevalent practice in medical ET is to use a sine or square excitation waveform with limited support on frequency-varied data acquisition.

Frequency selection and reconfiguration of excitation waveforms is a key factor for the experimentation in in vivo medical electrical tomography and advanced architectures are proposed [1] for respiration monitoring and diagnostic. Many methods are used in the optimization and analysis process [2-14]. In this document we present the emmiter design for a multifrequency electrical tomography device that complements the preliminary work of [1].

Impedance Spectroscopy

For biological tissues, current flow is not electronic but ionic. In electrochemistry, a mature measurement method is impedance spectroscopy (IS) and can be used to measure ionic, electronic and dielectric materials. IS [15] characterizes electrical properties of materials and their interfaces. The measurement principle in IS is similar to bioelectrical impedance [16, 17] analysis as it measures the variation of an excitation electrical signal applied to the system through electrodes over a range of frequencies.

Three excitation signals are generally used in IS to measure impedance:

1. *Step signal*. Transient measurements of the step response.

2. *Random white noise signal*. Comparison between the flat power spectra of white noise with respect to frequency dependent response of the output.

3. *Sine wave*. Measure phase-shift and change in amplitude or another method (e.g. fast Fourier transform) to obtain the real and imaginary parts of the impedance.

For the *step signal* excitation, a step voltage of u_0[V] is applied at time $t = 0$ and the output current $y(t)$[A] is measured. Transient measurements of the outputs need to be acquired under the supposition that the system has a linear response. From the control engineering point of view, the step response of the system is studied.

For the second excitation, *random white noise* $u_w(t)$ is sent as input signal, $u(t) = u_w(t)$. The spectrum of a white noise signal is expected to be flat over the frequencies, therefore frequency dependent variations in the output current $y(t)$ are the observed electrical response of the object under study.

For the third excitation, *sine wave* $u_\omega(t)$ is used as input, with constant frequency ω. With the output $y(t)$ measure the phase shift and amplitude variation and calculate the real and imaginary parts of the impedance. Given that the input signal is periodic, the fast Fourier transform (FFT) is well suited to estimate the impedance.

Measurement fundamentals

Impedance can be defined as the transfer function between an input flow and an output pressure [18]. If we have an excitation input flow $u(t)$ and a pressure output $y(t)$, then the impedance of the system is the transfer function:

$$Z(f) = \frac{\mathcal{L}\{y(t)\}}{\mathcal{L}\{u(t)\}} \tag{1}$$

With L the Laplace transform mapping the signals from timedomain to a complex frequency domain ($f \in \mathbb{C}$). In the electrical case, the input flow is current $I(t)$ and the output pressure is potential $V(t)$. If we measure the potential and current signals $V(t)$ and $I(t)$ for an electrically excited object, the impedance can be estimated directly from the (V,I) phase portrait. This method can account to identify non linear relations between (V,I), that is when $V = ZI$ is not followed by the system under measurement. In IS, the phase portrait is one of the oldest measurement method and is called Lissajous curves [19], because when the excitation signals are sinusoidal, the phase portrait can be described as a Lissajous curve where the shape of the ellipsoid is related with the phase shift of I with respect to V. In electronics, the (V,I) phase portrait is used in *analog*

signature analysis where a reference signature ($V_c(t)$,$I_c(t)$) is compared with the signature of a device under test to identify defaults [20, 21].

In practice it is also possible to estimate Z on-line using the ratio of the the estimated cross power spectral density S_{uy} and the power spectral density S_{uu}, in the case of current excitation u and potential response y [22]:

(2)
$$\hat{Z}(f) = \frac{\hat{S}_{uy}(f)}{\hat{S}_{uu}(f)}$$
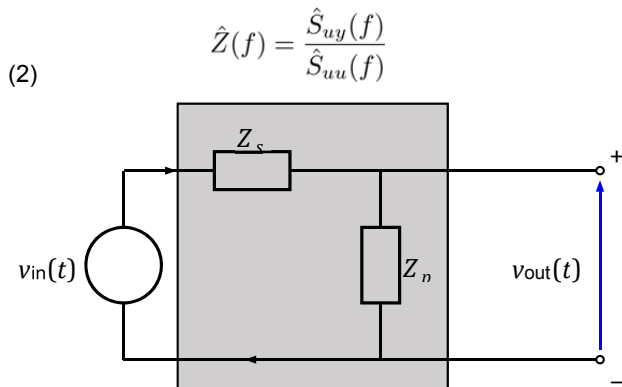
Fig. 1. Measurement set-up for impedance estimation methods.

A wide-range of methods for measuring impedance are available, that are generally combination of the methods stated before. In [23] the single sine, multisine and notably the chirp signal impedance measurement are presented and discussed. In the work of [24], a cost-effective electrical impedance spectrometer is presented using a narrow excitation pulse, a digital oscilloscope and FFT techniques.

To display the base elements for impedance estimation, the simple set up of Fig. 1 is presented. In the figure, Z_s is called output impedance, that is the impedance with respect to the source $v_{in}(t)$. Correspondingly, Z_p accounts for the input impedance, that is the impedance with respect of the input of the measuring system.

From Impedance Measurement to Tomography

Electrical impedance tomography is based in a parallel process of emission of an excitation signal $u(t)$ to a pair of electrodes on the surface of the object under study and at the same time the measurement $y(t)$ of a sample in a pair of electrodes localized anywhere on the surface. The observed impedance Z_{obs} can be estimated considering every measurement as a specific realization of the set-up of Fig. 1.

In standard tomography with sine wave excitation, if the excitation signal is provided by an electrical potential controlled source then the measured signal will be the current response, and correspondingly with a current controlled source the measurement signal will be the potential response.

The excitation-sensing measurement of impedance is repeated for many samples at different location for excitation electrode pairs and sensing electrode pairs. A global perspective of the state-of-the-art of EIT focused in complete pipeline from tissue to image is presented in [25].

Specific methods are reported in the literature to select excitation and sensing schemes (e.g. opposition, neighboring) that can be useful for one case and ineffective for other. The selection of a particular data acquisition scheme need to be justified with empirical data and specific modeling of the particular case.

Multi frequency electrical tomography

The goal of the data acquisition scheme is to collect enough surface response data for inference of the internal electrical conductivity distribution of the element under study. Considering a specific design of the emitter, the impedance measurement can be done using the same excitation signal in a range of frequencies. This is an interesting extension of the base electrical impedance tomography (EIT) method and it is called multi-frequency electrical tomography [26-29]. It is important to remark that multi frequency ET it can be considered as a multi-input multi-output IS method. That enables not only imaging but tissue identification: complex materials with non-linear response to frequency excitation and can be identified and isolated by its particular frequency response. Another advantage of using multi frequency techniques is validation using IS [30], because high precision IS measurement devices are available. There is a plethora of studies using multi frequency ET for complex tissues like in breast abnormality detection [31, 32], head imaging [33, 34], or for combined analysis like the obesity and heart diseases [35].
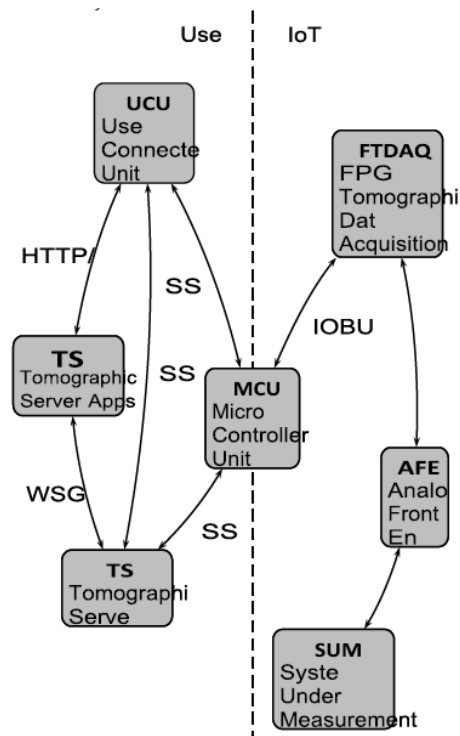
Fig. 2. Medical monitoring platform, building blocks.

The advancement on data acquisition technology correlates with the rise of applications for multi-frequency methods, given the possibilities of modern mixed signals integrated circuits with high speed, accuracy, and full dynamic range. For system integration in the wide sense, it comes with the challenge of the construction of new simulation schemes for the forward model under shape and frequencychanging patterns, and also for the image reconstruction for inverse solution estimation. The use of specific reconstruction methods are required because the techniques of traditional EIT will not benefit from the incorporation of the frequency dependent information [36].

IoT Monitoring Platform for Medical ET

The scheme of Fig. 2 present the fundamental elements for the medical ET monitoring platform design with IoT devices and services. The **UCU** block represent the user connected unit: the personal user networked device

(Laptop, Phone, Tablet) with wide area network connectivity (internet). We consider two types of users, clients and experts. Clients can access to the **TSA** block, the tomographic server-side applications using the web interface. The experts, that can connect directly to the **TS** block, the tomographic server where the tomographic raw data is available using secure shell communication (SSH).

The digital design was programmed in VHDL and the TAPI was programmed in Python in the MCU side. To reduce connection complexity, the tomographer was designed considering 16 dedicated excitation and sensing electrodes:

- 4 positive excitation electrodes ($I+$).
- 4 negative excitation electrodes ($I-$).
- 4 positive sensing electrodes ($V+$).
- 4 negative sensing electrodes ($V-$).

The MCU is a quad-core ARM Cortex based SoC, from Broadcom that provide wireless IoT connectivity to the de vice. The FPGA device is a XC3S1400AN from Xilinx, with 1.4M logic gates.

The mixed signal elements of the AFE are:

- DAC of 8bit, 4 channel multiplexed with SPI interface.
- ADC of 8bit, 4 channel multiplexed with SPI interface.

The ADC/DAC are driven at its maximum SPI clock speed of 40MHz. The resolution and the speed of the ADC/DAC are not of high grade and can be upgraded to more performing and compatible converters.
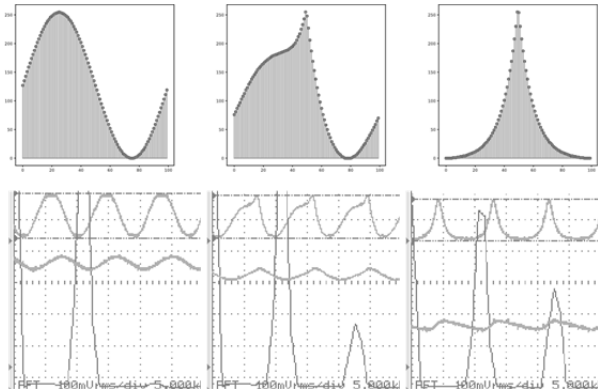
Fig. 3. In the first row are presented the quantized waveforms that were loaded in the T-RAM. In the second row are the raster images of the waveforms at 11.36kHz. Blue line is excitation with 2V per divide. Red line is the response with 500mV per divide. Green line is the FFT of excitation, with 100mV RMS per divide in the amplitude and 5kHz per divide in the horizontal axis.

Excitation Waveform Exploration

In order to show the results on the emitter and to avoid the effect of amplifiers and signal conditioning in the measurement we use the setup of Fig. 1 with the following parameters: a pure resistor $R = 218.6[\Omega]$ for Z_s and for Z_p we select a capacitor of 1[μF]. The objective of the test is not to measure impedance itself, that implies to introduce a reference impedance to measure current from a sensed potential (correspondingly, measure potential from a sensed current), but to test the emitter studying their potential response given a measured potential excitation with the minimal quantity of elements.

To study the effect of waveform reconfiguration, we measure the potential response of the system under three different excitation waveforms of the same designed amplitude and frequency, but with different energy. In the first row of Fig. 5 the quantized waveforms loaded into T-RAM are presented. The second row displays the measured excitation signals and their responses.

The first column of Fig. 3 shows the response of the sine wave, the third column of an exponential wave and the

second column is a sine+exponential wave. In this manner, the signals are presented from left to right in decreasing order of energy. Some important points can be observed directly from the plots:

- The DC level of the response correlates with the energy carried by the signal.
- The phase shift of the response also correlates with the energy.
- The sine wave response is shape preserving.
- The asymmetric excitation pattern of sine+exponential wave generates a symmetric pattern.
- The symmetric excitation pattern of the exponential wave generates an asymmetric pattern.

To get more insight, in Fig. 6 the response of six excitation waveforms were compiled. The leftmost first column displays a snapshot of 0.16 [ms] of the timeseries, sufficient time to display one complete period (1.8176 times the period). The blue line is used for the excitation input and the red for the sensed response. In the second column is located the input-output phase portrait (u,y). The trajectory of the system is time-colored from blue to yellow to show the evolution of the system during the data acquisition process. For the first and second columns, the excitation and the response were scaled to (0,1) to focus in shape and in time lag. The power spectral density (PSD) of the signals is compiled in a log-log plot in the third column, using again blue for excitation and red for response. The first peak of the PSD corresponds to the designed frequency of 11.36kHz for all signals.

Conclusions

Multi-frequency and waveform reconfigurable electrical data acquisition methods and practices can be included into electrical tomography. This is of particular importance in the *in vivo* measurement case: with a wider choice of parameters for controlling and designing data acquisition procedures, safe acquisition with precise data can be provided. Also, flexible pipelines of tomographic reconstruction can be visualized. Signal processing pipelines can be a helpful abstraction for incorporation of adaptive methods where the imaging data acquisition process is reconfigured to reflex the changes of the subject under study and/or when environmental conditions changes.

We develop the digital architecture of a system for multifrequency electrical tomography with re-configurable excitation waveforms. This implies the digital design of the emitter that replaces the general purpose, direct digital synthesis (DDS) integrated circuit and its analog counterparts used in standard electrical tomography, for an embedded device running in a FPGA. This choice allows to full control the emitter for excitation: it is possible to change dynamically the energy of the signal without changing the frequency or amplitude of the excitation, or to test the response of the system with different excitation waveforms.

Authors: *Tomasz Rymarczyk, Ph.D. Eng., University of Economics and Innovation, Projektowa 4, Lublin, Poland/ Research & Development Centre Netrix S.A. E-mail: tomasz@rymarczyk.com; Andres Vejar, Ph.D., University of Economics and Innovation, Projektowa 4, Lublin, Poland/ Research & Development Centre Netrix S.A. E-mail: andres.vejar@netrix.com.pl;*

REFERENCES

[1] Rymarczyk T., Vejar A., Multi frequency electrical tomography with re-configurable excitation waveforms, 2019 Applications of Electromagnetics in Modern Engineering and Medicine, PTZE 2019, 2019, 198-202

[2] Dušek J., Hladký D., Mikulka J., Electrical Impedance Tomography Methods and Algorithms Processed with a GPU, In PIERS Proceedings, 2017, 1710-1714.

[3] Korzeniewska E., Walczak M., Rymaszewski J., Elements of Elastic Electronics Created on Textile Substrate, Proceedings of the 24th International Conference Mixed Design of Integrated Circuits and Systems, MIXDES 2017, 447-45.

[4] Kryszyn J., Smolik W., Toolbox for 3d modelling and image reconstruction in electrical capacitance tomography, Informatyka, Automatyka, Pomiary w Gospodarce i Ochronie Środowiska (IAPGOŚ) , 7 (2017), No. 1,137-145.

[5] Nowakowski J., Ostalczyk P., Sankowski D., Application of fractional calculus for modelling of two-phase gas/liquid flow system, Informatyka, Automatyka, Pomiary w Gospodarce i Ochronie Środowiska (IAPGOŚ) , 7 (2017), No. 1, 42-45.

[6] Rymarczyk T., Characterization of the shape of unknown objects by inverse numerical methods, Przegląd Elektrotechniczny, 88 (2012), No 7b, 138-140

[7] Rymarczyk T., Adamkiewicz P., Polakowski K., Sikora J., Effective ultrasound and radio tomography imaging algorithm for two-dimensional problems, Przegląd Elektrotechniczny, 94 (2018), No 6, 62-69

[8] Rymarczyk T., Szumowski K., Adamkiewicz P., Tchórzewski P., Sikora J., Moisture Wall Inspection Using Electrical Tomography Measurements, Przegląd Elektrotechniczny, 94 (2018), No 94, 97-100

[9] Rymarczyk T., Tchórzewski P., Sikora J.: Implementation of Electrical Impedance Tomography for Analysis of Building Moisture Conditions, Compel The international journal for computation and mathematics in electrical and electronic engineering, 37 (2018), No. 5, 1837-1861

[10] Vališ, D., & Mazurkiewicz, D. (2018). Application of selected Levy processes for degradation modelling of long range mine belt using real-time data. Archives of Civil and Mechanical Engineering, 18 (2018), No. 4, 1430-1440.

[11] Kowalska A., Banasiak R., Romanowski A., Sankowski D., Article 3D-Printed Multilayer Sensor Structure for Electrical Capacitance Tomography, 19 (2019), Sensors, 3416

[12] Galazka-Czarnecka, I.; Korzeniewska E., Czarnecki A. et al., Evaluation of Quality of Eggs from Hens Kept in Caged and Free-Range Systems Using Traditional Methods and Ultra-Weak Luminescence, Applied sciences-basel, 9 (2019), No. 12, 2430.

[13] Rymarczyk T, Kłosowski G. Innovative methods of neural reconstruction for tomographic images in maintenance of tank industrial reactors. Eksploatacja i Niezawodnosc – Maintenance and Reliability, 21 (2019); No. 2, 261–267

[14] Rymarczyk, T.; Kozłowski, E.; Kłosowski, G.; Niderla, K. Logistic Regression for Machine Learning in Process Tomography, Sensors, 19 (2019), 3400.

[15] Macdonald J. R. and Johnson W. B., Fundamentals of Impedance Spectroscopy, ch. 1, 1–26. John Wiley & Sons, Ltd, 2005.

[16] Sanchez B., Vandersteen G., Martin I., Castillo D., Torrego A., Riu P. J., Schoukens J., and. Bragos R., In vivo electrical bioimpedance characterization of human lung tissue during the bronchoscopy procedure. a feasibility study, Medical Engineering & Physics, vol. 35, no. 7, pp. 949 – 957, 2013.

[17] Kusche R., Klimach P., and Ryschka M., A multichannel realtime bioimpedance measurement device for pulse wave analysis, IEEE Transactions on Biomedical Circuits and Systems, vol. 12, pp. 614–622, June 2018.

[18] Curran-Everett D., Zhang Y., Jones M. D., and Jones R. H., An improved statistical methodology to estimate and analyze impedances and transfer functions, Journal of Applied Physiology, vol. 83, no. 6, pp. 2146–2157, 1997. PMID: 9390993.

[19] Lasia A., Electrochemical impedance spectroscopy and its applications, in Modern Aspects of Electrochemistry (B. E. Conway, J. O. Bockris, and R. E. White, eds.), pp. 143–248, Boston, MA: Springer US, 2002.

[20] Pan H. and Yu S., A reconfigurable pcb test system based on vi, in 2011 International Conference on Electric Information and Control Engineering, pp. 91–94, IEEE, 2011.

[21] Neumann P., Pospíšilík M., Skocík P., and Adámek M., Theˇ iv characteristic comparison method in electronic component diagnostics, in 20th IMEKO World Congress 2012, 2012.

[22] Piret H., Granjon P., Guillet N., and Cattin V., Tracking of electrochemical impedance of batteries, Journal of Power Sources, vol. 312, pp. 60 – 69, 2016.

[23] Bullecks B., Suresh R., and Rengaswamy R., Rapid impedance measurement using chirp signals for electrochemical system analysis, Computers & Chemical Engineering, vol. 106, pp. 421 – 436, 2017. ESCAPE-26.

[24] Lewis G. K., Lewis G. K., and Olbricht W., Cost-effective broad-band electrical impedance spectroscopy measurement circuit and signal analysis for piezo-materials and ultrasound transducers, Measurement Science and Technology, vol. 19, p. 105102, aug 2008.

[25] Adler A. and Boyle A., Electrical impedance tomography: Tissue properties to image measures, IEEE Transactions on Biomedical Engineering, vol. 64, pp. 2494–2504, Nov 2017.

[26] Riu P., Rosell J., and Pallàs-Areny R., In vivo static imaging for the real and the reactive parts in electrical impedance tomography using multifrequency techniques, in 1992 14th Annual International Conference of the IEEE Engineering in Medicine and Biology Society, vol. 5, pp. 1706–1707, Oct 1992.

[27] Oh T. I., Woo E. J., and Holder D., Multi-frequency EIT system with radially symmetric architecture: KHU mark1, Physiological Measurement, vol. 28, pp. S183–S196, jun 2007.

[28] Oh T. I., Wi H., Kim D. Y., Yoo P. J., and Woo E. J., A fully parallel multi-frequency EIT system with flexible electrode configuration: KHU mark2, Physiological Measurement, vol. 32, pp. 835–849, jun 2011.

[29] McEwan A., Romsauerova A., Yerworth R., Horesh L., Bayford R., and Holder D., Design and calibration of a compact multifrequency EIT system for acute stroke imaging, Physiological Measurement, vol. 27, pp. S199–S210, apr 2006.

[30] Oh T. I., Koo H., Lee K. H., Kim S. M., Lee J., Kim S. W., Seo J. K., and Woo E. J., Validation of a multi-frequency electrical impedance tomography (mfEIT) system KHU mark1: impedance spectroscopy and time-difference imaging, Physiological Measurement, vol. 29, pp. 295–307, feb 2008.

[31] Halter R. J., Hartov A., and Paulsen K. D., A broadband high-frequency electrical impedance tomography system for breast imaging, IEEE Transactions on Biomedical Engineering, vol. 55, pp. 650–659, Feb 2008.

[32] Soni N. K., Hartov A., Kogel C., Poplack S. P., and Paulsen K. D., Multi-frequency electrical impedance tomography of the breast: new clinical results, Physiological Measurement, vol. 25, pp. 301–314, feb 2004.

[33] Yerworth R. J., Bayford R., Brown B., Milnes P., Conway M., and Holder D. S., Electrical impedance tomography spectroscopy (eits) for human head imaging, Physiological measurement, vol. 24, no. 2, p. 477, 2003.

[34] Romsauerova A., McEwan A., Horesh L., Yerworth R., Bayford R. H., and Holder D. S., Multi-frequency electrical impedance tomography (EIT) of the adult human head: initial findings in brain tumours, arteriovenous malformations and chronic stroke, development of an analysis method and calibration, Physiological Measurement, vol. 27, pp. S147–S161, apr 2006.

[35] Zhang S. X., Electrical Impedance Based Spectroscopy and Tomography Techniques for Obesity and Heart Diseases. PhD thesis, California Institute of Technology, 2017.

[36] Packham B., Koo H., Romsauerova A., Ahn S., McEwan A., Jun S. C., and Holder D. S., Comparison of frequency difference reconstruction algorithms for the detection of acute stroke using EIT in a realistic head-shaped tank, Physiological Measurement, vol. 33, pp. 767–786, apr 2012.